


湖南大学学报（自然科学版）
Journal of Hunan University (Natural Sciences)

第 50 卷 第 5 期
2023 年 5 月

Available online at <http://joununs.com/index.php/journal/index>

Vol. 50 No. 5
May 2023

Open Access Article

 <https://doi.org/10.55463/issn.1674-2974.50.5.8>

The Geochemical Character of Trace Elements in Coastal Sediments: Potential Implications of Metallic Mineral Resources on the West Coast of South Sulawesi, Indonesia

Adi Tonggiroh*

Department of Geological Engineering, Faculty of Engineering, Hasanuddin University, Makassar, Indonesia

* Corresponding author: adi.tonggiroh19@gmail.com

Received: February 16, 2023 / Revised: March 8, 2023 / Accepted: April 4, 2023 / Published: May 31, 2023

Abstract: This study aims to analyse the distribution model of trace elements and project alternative data on metallic mineral potential in the South Sulawesi Island by including grain distribution in nearshore sediments associated with river sediments. A total of 19 coastal sediment samples and 13 stream sediment samples were analysed by Inductive Coupled Plasma-Olyscope Emission Spectrophotometry (ICP-OES) for Cu, Pb, Zn, Ni, Co, Th, Sr, V, Cr, Ba, Nb, Rb, and Zr. Furthermore, this elemental collection was analyzed using Principal Component Analysis (PCA) and Pearson Correlation (PC) to understand the potential implications of critical minerals and a new distribution model of trace elements on geochemical characteristics related to the geogenic source. The results showed that the coastal sediments are enriched by Sr, Zn, V, Th, Rb, Ni, Nb, Cr, Cu, and Ba, but have a depletion of Co and Zr. Geochemical processes indicated by PCA Factor 1 consisting of Ba, Nb, Pb, Rb, Sr, Th, and Zr reflect metamorphic rocks, sulfate deposits in the Tonasa Formation sediments, Mallawa Formation, and natural or anthropogenic contamination. Factor 2, consisting of Co, Cr, Cu, Ni, V, and Zn, reflects dacite sulfide mineralization, intrusive rock, metamorphic, mafic-ultramafic, and magmatism forming land that then experiences recycling of older sedimentation. Many critical metallic minerals in river and coastal sediments have the potential as future economic resources, leading to the trend of coastal sediments (paleosediment).

Keywords: petrology, geochemistry, coastal sediments.

沿海沉积物中微量元素的地球化学特征：印度尼西亚南苏拉威西西海岸金属矿产资源的潜在意义

摘要：本研究旨在通过包括与河流沉积物相关的近岸沉积物中的颗粒分布来分析微量元素的分布模型并预测南苏拉威西岛金属矿产潜力的替代数据。采用电感耦合等离子体溶镜发射分光光度法(ICP-直读光谱仪)分析了总共 19 个沿海沉积物样品和 13 个河流沉积物样品中的铜、铅、锌、你、钴、钍、铈、V、铬、巴、铌、铷、锆。此外，还使用主成分分析(主成分分析)和皮尔逊相关(个人电脑)分析了该元素集合，以了解关键矿物的潜在影响以及微量元素的新分布模型对与地源相关的地球化学特征的影响。结果表明，沿海沉积物富集了铈、锌、V、钍、铷、你、铌、铬、铜和巴，而贫化了钴和锆。由巴、铌、铅、铷、铈、钍和锆组

成的主成分分析因子 1 指示的地球化学过程反映了变质岩、Tonasa 组沉积物、马拉瓦组中的硫酸盐沉积物以及自然或人为污染。因子 2 由钴、铬、铜、你、V 和锌组成，反映了英安岩硫化物矿化、侵入岩、变质岩、镁铁质-超镁铁质和岩浆作用形成的土地，然后经历了旧沉积物的循环。河流和海岸沉积物中的许多关键金属矿物具有作为未来经济资源的潜力，导致了海岸沉积物（古沉积物）的趋势。

关键词：岩石学、地球化学、沿海沉积物。

1. Introduction

The beach is a functional link between land and sea, which receives sediments carried by river currents and runoff from the land. The deposition of river sediments can be distributed along the coastline. This is influenced by waves, coastal currents, wind, climate, relief, and source composition [1]-[2]. Wave dynamics lead to geochemical processes that deposit trace elements in coastal sediments [3]. Sediments originating from land contain economic or non-economic value elements. Several types of minerals that have economic value are quartz, cassiterite, magnetite, ilmenite, and rare earth elements (zirconium, yttrium, barium, and strontium) [4].

South Sulawesi Province, Indonesia, is located on the southwestern arm of Sulawesi Island. Furthermore, it has a total coastline of 1,937 km, 288 km of which is located on the west coast of the main island. This region contains several types of important minerals including gypsum, nickel, silver, copper, and lead.

Deposits of major and trace elements in the South Arm of Sulawesi generally come from weathering of volcanic rocks [5]. Based on previous reports, the rocks found on the coast of the South Arm of Sulawesi are ultramafic and intrusive types [6]-[7]. This is consistent with previous studies that reported the outcrop of ultramafic, metamorphic, sedimentary and magmatism basement rocks as regional geological features of the South Arm of Sulawesi [8].

Among the exposed rock formations in this area, there are mineralized rocks that possibly originate from rivers. However, the origin in the arrangement of the coastal sediment mineral exploration is not necessarily directly related. The abundance of trace elements in river sediments is an indicator of the source composition [9]. Hence, the trace element studies must compare the composition and types of minerals on the coast and in rivers.

Coastal sediments offer several advantages as a source of ore deposits [10], associated minerals and their grain size distribution in the beach [11, 44], and coastal paleogeography related to heavy mineral concentrations [12]. The mineral composition of source rocks naturally exerts primary control over the accumulation of mineral constituents at any coastline

[13].

Due to the variety of rock formations exposed in the western part of Sulawesi Island, mineralized rocks are also found. Therefore, this study is based on trace elements and metallic minerals that are likely transported to rivers and beaches. Combined effects of chemical, biological and physical weathering processes transform bedrock into soils and ultimately into sediments [14]. The chemical composition of the source magma and the physicochemical conditions of the depositional environment are the main controlling factors in determining the behavior and mobility of trace elements and REEs during transformation [15].

This study provides an overview of the potential and distribution of metallic minerals in the South Arm of Sulawesi based on the geochemistry of Ba, Co, Cr, Cu, Nb, Ni, Pb, Rb, Sr, Th, V, Zn and Zr in nearshore sediments and controls mineralized source rock in river sediment elements. The novelty expected from this study is the finding regarding the origin of trace elements in rock formations at the study site.

Geochemical knowledge of the distribution and migration of elements is crucial to identifying their origin [16]. Some beach placer deposits formed by waves and currents transported the shelf sands and concentrated the ore minerals [17]. Therefore, this study aims to analyse the distribution model of trace elements and project alternative data on metal mineral potential in the South Arm of Sulawesi Island by including grain distribution in nearshore sediments associated with river sediments.

2. Materials and Methods

The geographical location of the nearshore sediment study area is opposite the Makassar strait and is included in the regional geology of western Sulawesi [6,18]. It has a coastline of about 10 km as well as an urban city (Parepare) in the northern part and Barru-Pangkajene area in the southern part, where both have varied erosion and sedimentation. The study location was chosen because western Sulawesi has high mineral potential, which can be explored for the benefit of exploiting natural resources.

In the study area, volcanic rocks of the Parepare Formation, sedimentary rocks of the Tonasa Formation

(Limestone and marl), Mallawa Formation (quartz sand, conglomerate, siltstone, and claystone with coal insertion), dacite, diorite, and ultramafic rocks are exposed on the land surface. This region experiences the seasons of the west monsoon from December to March and the east monsoon from June to October. Beach sediments were poorly sorted during the postmonsoon, and their grain size was coarser at this time than in the monsoon period [19]. The sampling of rock minerals was carried out along 24 km of the coastline and surrounding rivers. A total of 32 samples were divided into two types of sources, namely 19 samples on coastal sediments and 13 on sediments of the Binangae River (Salo Binangae) and surrounding rivers (Figure 1).

Coastal sediment sampling was carried out from April to November 2019 with the continuity of sampling points following the coastline. Each point of the beach sediment sample was obtained from the channel in the foreshore zone using a hand trowel, where the horizontal direction was ± 20 cm and the vertical direction was at a depth of 0 – 30 cm (Figure 2). In addition, the collected sand and minerals were then put into polyethylene bags. River sediment samples were obtained from the top layer composite to the bottom using a sieve of 80 to 200 mesh size and then put inside a polyethylene bag. The beach width and slope were measured using linen tape and a clinometer, respectively.

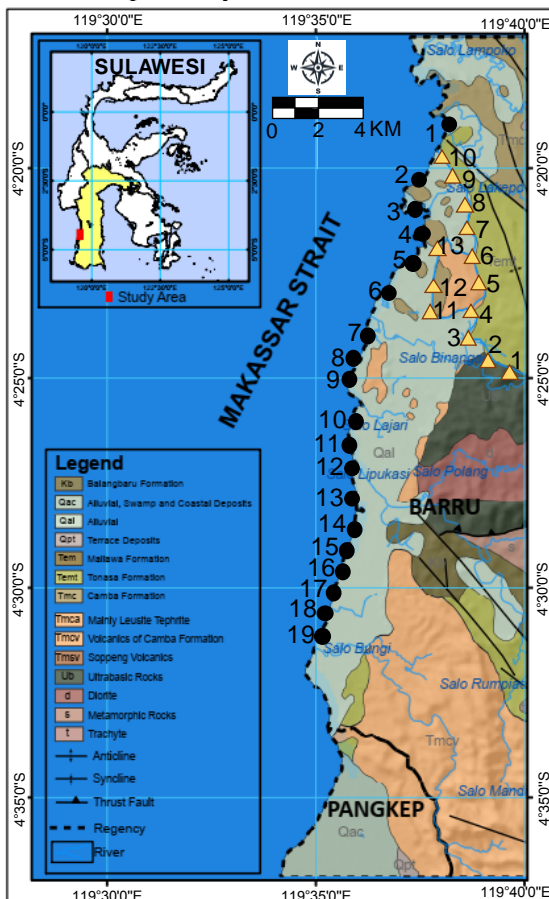


Fig. 1 Distribution of sampling points at study sites in Sulawesi Arm (Modified from Regional Geological Map⁷)

Coastal sediment sampling was carried out from April to November 2019 with the continuity of sampling points following the coastline. Each point of the beach sediment sample was obtained from the channel in the foreshore zone using a hand trowel, where the horizontal direction was ± 20 cm and the vertical direction was at a depth of 0-30 cm (Figure 2).



Fig. 2 AC – Morphology and coastal sediment in locations 1 to 8; BD – Morphology and coastal sediment in locations 9 to 19

In addition, the collected sand and minerals were then put into polyethylene bags. River sediment samples were obtained from the top layer composite to the bottom using a sieve of 80 to 200 mesh size and then put inside a polyethylene bag. The beach width and slope were measured using linen tape and a clinometer, respectively.

Coastal sediment samples were prepared at the Sedimentology Laboratory of the Geology Department, Hasanuddin University. The samples were dried in an oven at a temperature of 100°C for 3 hours, followed by grain size and mineralogy analysis. Grain size analysis was carried out using a Retsch AS 200 vibratory sieve shaker according to the American Society for Testing and Materials (ASTM) with sieves ranging from 1.5 to 4.25 at 0.50 intervals for 20 minutes. The sample mineralogy was analysed using a binocular microscope with 100x magnification on a 0.150 mm mineral mesh. Trace elements in coastal sediment samples were detected using Inductively Coupled Plasma-Optical Emission Spectrophotometry (ICP-OES), with a detection limit of 1 ppm, except for Nb 0.1 ppm, Sr 0.5 ppm, and Th 0.05 ppm. The main steps of the research process are summarized in Figure 3.

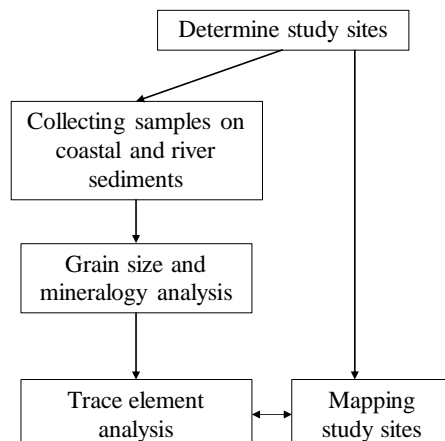


Fig. 3 Summarized study stages

Chemical data of coastal and river sediment samples were analyzed using multivariate statistical methods, which have been widely employed in the geological field, specifically in segments that deal with many variables, such as petrology and sediment geochemistry [20]. The result was an array of data in which elements were grouped as associations through their correlation coefficients or other measures of association [21]. Multivariate analysis was conducted on trace elements using PCA statistics to capture correlated data structures [22] and multivariables [23], and to determine source dominance and trace element correlations [24]. Each variable for 13 elements was selected using eigenvalue > 1, leading to the first extraction factor (F1) with a total variance of 71.75% and eigenvalue of 8.254, while the second factor (F2) total variance was 21.558% with an eigenvalue of 2.803. Rotation of both generated three highly correlated variables (cut-off point = 0.55) with a factor of 1 (0.794; 0.864; 0.895; 0.972; 0.07; 0.961; 0.921), namely Ba, Nb, Pb, Rb, Sr, Th, and Zr. Meanwhile, there are also highly correlated variables for factor 2 (0.353; 0.19; 0.663; 0.172; 0.658; 0.802), namely Co, Cr, Cu, Ni, V, and Zn.

3. Results and Discussion

3.1. Grain Size Analysis

The results showed that the sand component was fine to medium in size with three statistical differences (Table 1). First, samples 1 to 8 consisted of sand ($\pm 93.13\%$), silt ($\pm 6.816\%$), and clay ($\pm 0.006\%$), with a mean of 0.5-0.6, variance (σ) of 0.5-0.7, skewness of 0.3-0.7, and kurtosis of 1.0-2.0. Samples 1 to 8 were positioned near the mouths of several rivers, hence, the presence of minerals in these locations was related to sedimentation from rivers and the small influence of waves (Figure 3AC). Second, samples 9 to 13 were located in the middle and composed of sand ($\pm 98.39\%$), silt ($\pm 0.12\%$), and clay ($\pm 0.00\%$), with a mean of 0.09–0.16, variance (σ) of 0.03–0.06, skewness of 0.62–0.4, and kurtosis of 0.75–1.72. At this location, the influence of sedimentation and irregular waves moved to the north. Third, samples 14 to 19 contained sand ($\pm 93.9\%$), silt (± 3.595), and clay ($\pm 2.050\%$), with a mean of 0.12-0.04, variance (σ) of 0.05-0.68, skewness of 0.04-0.65, and kurtosis of 0.52-3.36, while their locations were quite far from the river mouth. The results of this mineral observation indicated that the grain distribution and the waves' influence were moderate to the south (Figure 3BD).

The analysis confirms previously identified trends of increasing beach face slope with increasing sediment grain size and decreasing beach exposure to wave energy [25]. Meanwhile, wind-generated waves are the prime sources of energy driving sediment discharge, beach morphology, and breaker waves [26]. The

change in the west and east monsoons in Sulawesi occurs every six months, but strong changes occur within three months (BMKG). This causes erosion and sedimentation to vary on the west coast of South Sulawesi [27].

Table 1 The percentages of the sediment components

Group	Mean (mm)	Sands (%)	Silt (%)	Clay (%)
01	0.06	89.79	10.20	0.01
	0.62	89.79	10.21	0.00
	0.56	99.80	0.19	0.01
02	0.09	99.80	0.20	0.00
	0.16	96.97	0.03	0.00
03	0.12	88.83	7.17	4.00
	0.14	98.97	0.02	0.10

3.2. Mineralogical Analysis

The mineralogical analysis, which is related to the grain and wave distribution, is divided into three parts. First, the distribution of sedimentation grains in zone one consists of biotite (2-5%), plagioclase (30-50%), hornblende (15-40%), and opaque minerals (5-25%). These types of minerals are generally found in locations with small wave effects, and because the zone is close to the river, several plagioclases are present. The high plagioclase composition in the sand marks the weathering sedimentation of Parepare volcanic rocks, trachyte porphyry [28], while the opaque mineral content is probably generated by sediments transported from the south. Second, zone two consists of pyroxene (25-45%), quartz (15-25%), and opaque (5-10%) mineral content. The grain distribution at these locations is influenced by the direction of the irregular waves toward the north. Significant differences between pyroxene and quartz in the sand are ascribed to the weathering of acid-intermediate and ultramafic rocks. The opaque minerals promote the presence of heavy minerals from weathering of mineralized rocks possibly generated by sediments transported from the south. Third, zone two also consists of biotite (20-25%), pyroxene (15-25%), quartz (15-20%), orthoclase (10-20%), and opaque minerals (10-15%). The grain distribution at these locations is influenced by the direction of moderately irregular waves toward the south. The similarity in the quantities of biotite, pyroxene, quartz, and orthoclase indicates that the sand collects minerals originating from land and beaches.

Based on the mineral association group, the zones can be divided into two mineral distribution bands. In the first zone, mineral distribution to the north (samples 1 to 8) is dominated by plagioclase and hornblende (Figure 4A), while in zone 2, the distribution from north to south (samples 9 to 19) is dominated by pyroxene, quartz, and orthoclase (Figure 4CD).

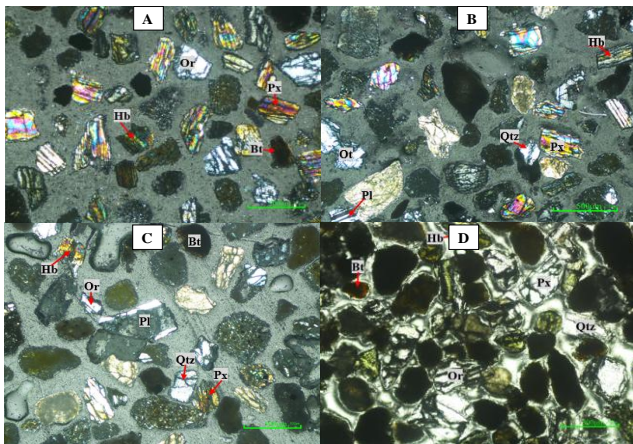


Fig. 4 A and B – Mineralogy in coastal sediment collection from locations 1 to 8; C and D – Mineralogy in coastal sediment collection from locations 9 to 19 (Magnification - 50 × nicol)

Plagioclase dominance in zone 1 is also influenced by mineral migration from the north originating from regional rocks with acidic chemical composition (Figure 4B), while the zone 2 source has an alkaline chemical composition. The mineral associations of zones 1 and 2 are different because the mentioned northern part shows mineral associations originating from a large variety of weathering and includes the northern part of the west coast of Sulawesi.

3.3. Geochemical Analysis of Beach Sediments

Referring to the normalized data of upper continental crust Co (17.3 ppm) and Zr (193 ppm) as stated by Taylor and McLennan SM (1985) based on all geochemical data of nearshore deposits, the overall results showed high concentrations of Sr, Zn, V, Th, Rb, Ni, Nb, Cr, Cu, Ba, Co, and Zr (Table 2).

Table 2 Trace element data (ppm) for the beach sands

Element	Mean	Variance	Skewness	Kurtosis	Min.	Max.
Cu	15.526	39.041	1.642	3.151	8.00	34.00
Pb	33.526	109.374	-0.842	-0.325	13.00	48.00
Zn	79.157	1156.585	1.963	3.354	47.00	177.00
Ni	36.105	367.988	0.925	0.334	15.00	84.00
Co	22.315	161.895	0.749	-0.317	9.00	50.00
Cr	126.000	4834.889	0.673	-1.061	53.00	254.00
Th	19.436	67.716	-0.442	-1.228	5.59	30.50
Sr	793.157	143.411.807	1.840	3.512	399.00	1880.00
V	178.421	18474.146	1.880	2.965	80.00	558.00
Ba	837.947	22.320.386	-0.309	-0.486	546.00	1070.00
Nb	16.305	52.102	-0.907	-0.147	2.20	25.80
Rb	122.731	2418.058	-0.629	-1.125	28.60	180.00
Zr	231.473	2863.041	-0.352	-0.749	134.00	315.00

High concentrations of elements indicate the role of sand-silt as a trap for elements that are then transported following river flow and deposited near the coast. This characteristic was reinforced by the relatively increased levels of Co (22,135 ppm) and Zr (231,473 pm). The chemical properties and deposition of Co in the sand may be associated with its low mobility because it is mostly derived from soluble minerals, while immobile Zr is highly adsorbed in the silt. The results show that several trace elements such as Sr, Ba, Nb and Zr are higher than previous studies [29]. Sr is commonly used to treat osteoporosis and toothache [30]. Ba in the form of barium sulfate has potential novel applications and wide use in polymer and paint industries [31]. Nb and Zr are commonly used for the production of high-temperature resistant metal alloys and special stainless steels [32]-[33]. The correlation between elements of high and low concentrations is also shown in the Pearson correlation coefficient data from 19 coastal sediment samples (Table 3). Some general groups of positively correlated elements are Ni, Cr, Co, Cu, and Zn. The positive correlation is an independent element reinforcement that states these two groups differ in their source of rock types. Furthermore, using the 0.01 level, the general group of positive correlations becomes the main group of elements to be observed, namely (1) Co vs Cr, Ni, Zn, and V, (2) Cu vs Zn and V, and (3) Pb vs Ba, Nb, Rb, Th, and Zr. This grouping produces Pb, Ba, Nb, Rb, and Th, which have similar rock sources, although there are differences in their similarities when correlated with high concentrations of Sr. Compared with Upper continental crust (UCC) normalized trace elements data, the difference in the similarity of Sr (399 ppm to 1880 ppm) indicates that the rock source contains K-feldspar originating from regionally acidic compositional rocks such as granite, granodiorite, diorite, and quartz monzonite. This inlined with other previous studies [34, 35]. Using significant dilution values reflecting the elements that have chemical mobility, Co (-0.21), Cu (-0.39), Nb (-0.40), Pb (-0.34), and Rb (-0.24) were obtained. The negative value reflects sand-silt traps originating from rivers and then deposited near the coast.

Table 3 The Pearson correlation analysis and coefficients of the beach sediments

	Cu	Pb	Zn	Ni	Co	Cr	Th	Sr	V	Ba	Nb	Rb
Cu	1											
Pb	0.076	1										
Zn	0.496*	-0.112	1									
Ni	0.008	-0.904**	0.295	1								
Co	0.288	-0.646**	0.775**	0.816**	1							
Cr	0.129	-0.809**	0.563*	0.840**	0.892**	1						
Th	-0.035	0.935**	-0.293	-0.933**	-0.799**	-0.897**	1					
Sr	-0.392	-0.349	-0.485*	0.125	-0.210	0.189	-0.255	1				
V	0.449	-0.341	0.962**	0.532*	0.907**	0.735**	-0.520*	-0.0379	1			
Ba	-0.226	0.733**	-0.418	-0.732**	-0.677**	-0.658**	0.669**	0.178	-0.555*	1		
Nb	0.098	0.951**	-0.025	-0.896**	-0.618**	-0.782**	0.959**	-0.405	-0.272	0.584**	1	
Rb	-0.049	0.952**	-0.307	-0.944**	-0.797**	-0.898**	0.983**	-0.243	-0.532*	0.772**	0.936**	1
Zr	-0.207	0.829**	-0.381	-0.876**	-0.803**	-0.761**	0.909**	0.031	-0.582**	0.719**	0.837**	0.900**

* Correlation is significant at the 0.05 level (2-tailed).

** Correlation is significant at the 0.01 level (2-tailed).

The main element group in the wave's variable direction toward the north (samples 1 to 8) has Pearson values which are dominated by V, Ni, Cr, Co, Cu, Pb, and Zn against Ba, Rb, Nb, Th, and Zr groups that are indicated to be abundant in clay. The high field strength elements Zr, Nb, and Th are good indicators of source rock characteristics [36]. A review of low Zr concentrations indicates that coastal deposits reflect the presence of intermediate rock mineralization, confirmed by the high spot Zn concentration and the distribution of Sr, V, Rb, and Zr (Figure 5). Meanwhile, from silt sediments near the coast and sedimentation in the south (Samples 9-19), positive Pearson correlations were obtained in the Ni, Cr, and Co as well as Cu, Zn, and V groups. This was achieved using high concentrations of Cu, Zn, and V generally derived from rocks with an acid composition such as volcanic rock (Figure 6). However, the results of the iteration of positive correlation and increasing Co concentration were linear with increasing Cr ($R^2 = 0.76$). The determination of Cr and Ni is highly correlated, indicating the source of rocks with an ultramafic composition.

PCA was used to reduce the effect of the number of data variables. This was conducted using factor extraction with an Eigenvalue > 1 after varimax rotation to obtain elemental groups in factors that provide some information about the distribution and source of mineralized rocks. The extraction results showed that the first component (F1) has an eigenvalue of 8.254, explaining the total variance of 63.50%. The second factor (F2) has an eigenvalue of 2.80, explaining the total variance of 21.56% (Table 4).

Table 4 PCA results for 13 elements

Component	Total	% of Variance	Cumulative %
1	8.254	63.50	63.50
2	2.803	21.56	85.05

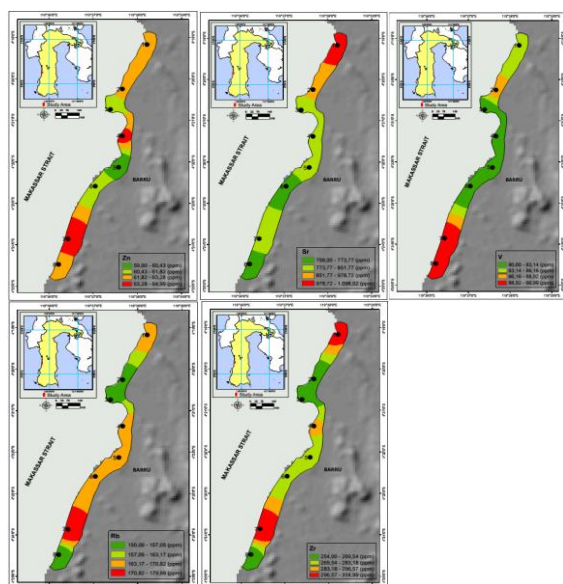


Fig. 5 Distribution and concentration of Zn, Sr, V, Rb, and Zr (samples from Locations 1-8)

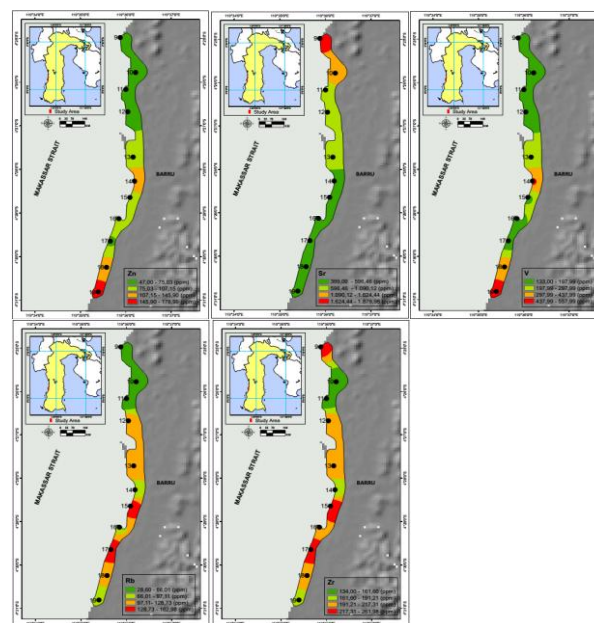


Fig. 6 Distribution and concentration of Zn, Sr, V, Rb, and Zr (samples from Locations 9-19)

Through rotation, the distribution of variables becomes clear and real; hence, the large loading factor increases and vice versa, compared to before this process. Two rotations of matrix components are produced according to the number of factors obtained, namely the distribution of variables into factors with rotation. Based on (Figure 7), the scree plot shows that after being rotated there are three highly correlated variables (cut off point = 0.55) with a factor of 1 (0.794; 0.864; 0.895; 0.972; 0.07; 0.961; 0.921), namely Ba, Nb, Pb, Rb, Sr, Th, and Zr. Meanwhile, for factor 2 (0.353; 0.19; 0.663; 0.172; 0.658; 0.802), namely Co, Cr, Cu, Ni, V and Zn, there are also highly correlated variables. Factor 1, which is the concentration of incompatible trace elements Nb, Pb, Rb, Sr, and Th, reflects a stable mineral assemblage originating from the metamorphism of the main hosts and metamorphic basement rock of new South Sulawesi [34].

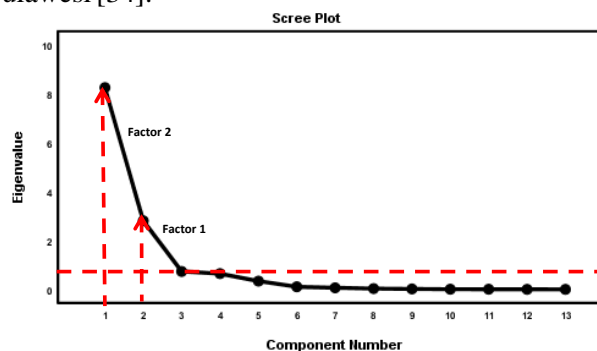


Fig. 7 Scree plot factors 1 and 2

In addition, Ba is from barium sulfate in the Tonasa Formation sediments [34] and Zr is an immobile element [37]. Trace element factor 2 at the concentration of Co, Cr, Cu, Ni, V and Zn in coastal

sediments implies mineral enrichment from intrusive, basaltic-ultramafic, ultramafic, harzburgite peridotite and podiform chromitite rock types as the basement rock of South Sulawesi [8]. Moreover, dacitic rocks [38] intrude the metamorphic and ultramafic sequences [39].

3.4. Geochemical Analysis of Stream and River Sediments

Table 5 The statistical description of stream sediment

Element	Mean	Variance	Skewness	Kurtosis	Min.	Max.	
Cu	34.538	394.769	-0.618	-1.381	5.00	58.00	Cu
Pb	18.307	124.564	1.652	3.549	5.00	48.00	Pb
Zn	122.769	6844.192	2.346	7.025	40.00	368.00	Zn
Ni	76.384	1159.756	0.079	-0.625	27.00	140.00	Ni
Co	44.846	1104.974	0.856	0.899	8.00	122.00	Co
Cr	913.538	2372281.936	2.740	8.100	18.00	5610.00	Cr
Th	4.450	9.186	0.660	-0.865	0.73	9.67	Th
Sr	479.776	45280.614	-0.385	0.380	55.10	841.00	Sr
V	333.538	144712.603	2.455	7.249	19.00	1470.00	V
Ba	548.3077	231242.397	1.349	2.250	37.00	1760.00	Ba
Nb	4.900	9.587	0.007	-1.015	0.60	9.70	Nb
Rb	36.530	1579.204	2.398	6.453	5.10	153.00	Rb
Zr	65.092	1922.041	-0.350	-1.899	6.60	114.00	Zr

The analysis results showed the difference in skewness strength and maximum concentration of the aforementioned elements. This is caused by the geochemical enrichment process, which is influenced by the variability of regional geological and sub-geological rocks of the study area, such as dacite, diorite, and ultramafic rock. Statistical differences also indicate that elements originating from rivers and coastal deposits can contain metallic mineral resources. Another study discovered high values of V and low values of Rb [40] as well as potential mineral resources and REEs. Out of the 13 elements, there are similarities between Nb, Rb, Th, and Zr with continental crust composition. Previous studies indicated that these elements come from weathering of riverine rock of diorite [41] and dacite [38].

The chemical properties of V and Zn, which are relatively high in coastal and river sediments, are used as a correlation between regional and sub-geological rock sources in the study area. There is a significant similarity in the high correlation coefficient of V vs. Zn (Figure 8AC) at the sampling point in the river ($R^2 = 0.897$) and the coast ($R^2 = 0.925$), reflecting the continuity of geochemical enrichment of mineral resource potential and REE, high values of V, and low values of Rb. Although Rb has a positive correlation coefficient, there is a significant difference between Rb vs Sr ($R^2 = 0.556$) in the river and Rb vs Zr ($R^2 = 0.810$) in the coast (Figure 8BD). Zr is sourced from igneous rocks of intermediate to acidic composition, while Sr characterizes igneous, metamorphic, and carbonate sedimentary rocks and filling fractures. The enrichment of Rb, Sr, and Zr was sourced from the Tonasa Fromasi sedimentary and intrusive rocks. Besides, fluvial systems of these river basins represent

Statistical characteristics of chemical data analysis on sediments of 13 sand and clay samples in the Binangae stream can be seen in (Table 5). Sources of the present elements are known from statistical comparisons of trace elements of coastal and river sediments. Rb, Sr, V, Zn, and Zr were found in river sediments, which were the same as the groups found on the coast (Table 5).

varied elevations, landscape patterns, precipitation, as well as physical and chemical denudation, which are all key controlling factors for the input of terrigenous sediments to the oceanic environment [42]. Pearson correlation of Ba, Co, Cr, Ni, Pb, Rb, V and Zn indicates a positive geogenic source absorbed by clay minerals in the sediment stream. Trace elements such as Sc, Th, Zr, Cr, Ni and Co are generally immobile during surficial [34]. Sources of Cu, Ni, and Sr from different rocks are considered to affect the distribution of other elements, specifically Zn, Pb, and V correlation reflecting sulfide mineralization. Meanwhile, the concentration of Ni, Cr, and Co is related to the mineralization of ultramafic rocks of Harzburgite peridotite and podiform chromitite [34], as well as very high concentrations of Ba (1760 ppm) associated with barite ($BaSO_4$) deposits in the Tonasa Formation [43]. This study was limited to locations on the West Coast of South Sulawesi and merely examined trace elements.

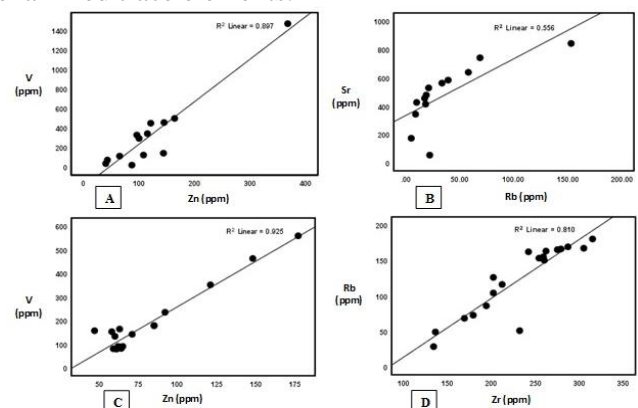


Fig. 8 A and B – Correlation between elements in river sediments; C and D – Correlation between elements in river and coastal sediments

4. Conclusion

Based on the results, 19 coastal sediment samples reflect trace elements more strongly sourced from northern regional geological rocks, while the 13 river sediment samples were sourced from regional sub-geological rocks where transitional elements accumulated within locations 8 and 9.

The higher the enrichment of Sr, Zn, V, Th, Rb, Ni, Nb, Cr, Cu and Ba, the more the depletion of Co and Zr concentrations was found in the coastal sediments. Possibly, the control of the beach sand composition was due to the influence of the river fluvial system on grain size characteristics, narrow coastal plains, and changes in coastal currents and waves. In addition, the coastal deflation process is critical to the redistribution of mafic and quartz mineralogy, which was concentrated along the coast to the south.

Ba, Nb, Pb, Rb, Sr, Th, and Zr occurred in metamorphic rocks, sulfate deposits in the Tonasa Formation sediments, Mallawa Formation, and natural or anthropogenic contamination. Meanwhile, while Co, Cr, Cu, Ni, V, and Zn occurred, sulfide mineralization occurred in dacite and mafic-ultramafic rocks

There were three concentration characteristics from the river to coastal sediments, where the concentration decreased with Ba, Co, Cr, Cu, Ni, V and Zn and increased with Nb, Rb, Sr, Th, Zr and Pb. The occurrence of this significant concentration correlated with the specific geology of the sub-study area, as well as the disintegration and mineralization of volcanic, intermediate, dacitic, Tonasa and Mallawa Formation, and ultramafic rocks. It also correlated with urban city development on the east side of the study area and the regional element supply of the Makassar Strait on the west side. In addition, many critical metallic minerals in river and coastal sediments that are potential future economic resources lead to a paleo-deposit trend sourced from volcanism, metamorphism, mineralization, and recycling of older sediments.

The results of this study have effectively answered the objectives because they have explained the distribution model of trace elements and project alternative data on metallic minerals potential in the South Sulawesi Island by including grain distribution in nearshore sediments associated with river sediments.

References

- [1] MALICK B M L, YOUNG L M, and ISHIGA H. Major and trace element geochemistry of beach sands from northern Kyushu, Japan. *Geoscience Reports of Shimane University*, 2012, 31: 1-8.
- [2] MALICK B M L, and ISHIGA H. Geochemical maturity of pocket beach sands from the San'in region of southwest Japan. *Earth Science Research*, 2015, 4: 74-84. <http://dx.doi.org/10.5539/esr.v4n2p74>
- [3] ALYAZICHI Y M, JONES B G, MCLEAN E, PEASE J, and BROWN H. Geochemical assessment of trace

- element pollution in surface sediments from the Georges River, Southern Sydney, Australia. *Archives of Environmental Contamination and Toxicology*, 2017, 72: 247-259. <https://doi.org/10.1007/s00244-016-0343-z>
- [4] LONG K R, VAN GOSEN B S, FOLEY N K, and CORDIER D. The principal rare earth elements deposits of the United States: A Summary of Domestic Deposits and a Global Perspective". In: SINDING-LARSEN R, WELLMER FW. (Eds) *Non-Renewable Resource Issues. International Year of Planet Earth*. Springer, Dordrecht, 2012. https://doi.org/10.1007/978-90-481-8679-2_7.
- [5] WITASARI, Y. Composition and origin of clay minerals and trace elements in the recent sediments of Makassar Strait, Indonesia. Proceedings of the XIIIth International Conference on Researches in Science & Technology. Bali, Indonesia, 2454-5880, 2018.
- [6] MAULANA A, CHRISTY A G, and ELLIS D J. Petrology, geochemistry and tectonic significance of serpentinized ultramafic rocks from the South Arm of Sulawesi, Indonesia. *Chemie der Erde - Geochemistry*. 2014, 75(1): 73-87. <https://doi.org/10.1016/j.chemer.2014.09.003>
- [7] GODANG S, IDRUS A, FADLIN BP, and BASUKI NI. Sapolitization's Characteristics of Rare Earth Elements in Volcanic Regolith on Drill Core #65 in Western Sulawesi, Indonesia. *Asian Journal of Applied Science*, 2019, 7(4): 435-450. <http://dx.doi.org/10.24203/ajas.v7i4.5873>
- [8] WAKITA K, MUNASRI SOPAHELWAKA NJ, ZULKARNAEN I, and MIYAZAKI K. Early Cretaceous tectonic events implied in the time-lag between the age of radiolarian chert and its metamorphic basement in the Bantimala area, South Sulawesi, Indonesia. *Island Arc*, 1994, 3: 90-102. <https://doi.org/10.1111/j.1440-1738.1994.tb00097.x>
- [9] YOUNG S M, PITAWALA A, and ISHIGA H. Geochemical characteristics of stream sediments, sediment fractions, soils, and basement rocks from the Mahaweli River and its catchment, Sri Lanka. *Geochemistry*, 2013, 73: 357-371. <https://doi.org/10.1016/j.chemer.2012.09.003>
- [10] O'SULLIVAN G, CHEW D, KENNY G, HENRICHS I, and MULLIGAN D. The trace element composition of apatite and its application to detrital provenance studies. *Earth-Science Reviews*, 2020, 201: 103044. <https://doi.org/10.1016/j.earscirev.2019.103044>
- [11] JORDENS A, CHENG YP, and WATERS KE. A review of the beneficiation of rare earth element bearing minerals. *Minerals Engineering*, 2013, 41: 97-114. <https://doi.org/10.1016/j.mineng.2012.10.017>
- [12] ACHARYA B C, NAYAK B K, and DAS S K. Heavy mineral placer sand deposits of Kontiagarh area, Ganjam District, Orissa, India. *Resource Geology*, 2008, 59(4): 388-399. <https://doi.org/10.1111/j.1751-3928.2009.00105.x>
- [13] HOU B, KEELING J. and GOSEN B S. Geological and exploration models of beach placer deposits, integrated from case-studies of Southern Australia. *Ore Geology Reviews*, 2017, 80: 437-459. <https://doi.org/10.1016/j.oregeorev.2016.07.016>
- [14] PAPADOPOULOS A, TZIFAS IT, and TSIKOS H. The potential for REE and associated critical metals in coastal sand (Placer) Deposits of Greece. *Minerals*, 2019, 9(8): 469. <https://doi.org/10.3390/min9080469>
- [15] CHARLESWORTH S, DE MIGUEL E, and ORDONES A. A review of the distribution of particulate trace elements in urban terrestrial environments and its

- application to considerations of risk. *Environmental Geochemistry and Health*, 2011, 33(2): 103-123. <https://doi.org/10.1007/s10653-010-9325-7>.
- [16] NAMAYANDEH A, MODABBERI S, and LOPEZ-GALINDO A. Trace and Rare Earth Element Distribution and Mobility during Diagenetic Alteration of Volcanic Ash to Bentonite in Eastern Iranian Bentonite Deposits. *Clays and Clay Minerals*, 2020, 68(1): 50-66. <https://doi.org/10.1007/s42860-019-00054-9>
- [17] SITDIKOVA LM, IBRAGIMOV EA, BADRUTDINOV OR, KHASANOVA NM, and MUKHAMATDINOV, I. I. Material composition of coastal marine placer deposits of the Arabian sea coast (Kollam, Kerala, India). *International Multidisciplinary Scientific GeoConference: SGEM*, 2016, 1: 361-367.
- [18] PRAKASH T, BLACK K, MATHEW J, KURIAN NP, et al. Nearshore and Beach Sedimentary Dynamics in a Placer-Dominated Coast, Southwest India. *Journal of Coastal Research*, 2007, 23(6): 1391-1398. <http://www.jstor.org/stable/30138538>.
- [19] TONGGIROH A, KAHARUDDIN, PISIAS NG, MURRAY RW, and SCUDDER RP. Multivariate statistical analysis and partitioning of sedimentary geochemical data sets: General principles and specific MATLAB scripts: Technical Brief. *Geochemistry, Geophysics, Geosystems*, 2013, 14(10): 4015-402. <https://doi.org/10.1002/ggge.20247>
- [20] ALBANESE, S, CICHELLA, D, and DE VIVO, B. *Geochemical mapping of urban areas*, chapter 8, Environmental geochemistry site characterization, data analysis and case histories, 2017. <http://dx.doi.org/10.1016/B978-0-444-63763-5.00009-4>
- [21] IWAMORI H, YOSHIDA K, NAKAMURA H, KUWATANI T, et al. Classification of geochemical data based on multivariate statistical analyses: Complementary roles of cluster, principal component, and independent component analyses. *Geochemistry, Geophysics, Geosystems*, 2017, 18: 994-1012. <https://doi.org/10.1002/2016GC006663>
- [22] CHENG Q, CARTER G. B, WANG, W, ZHANG, S, LIE, W, and QINGLIN, X. A spatially weighted principal component analysis for multi-element geochemical data for mapping locations of felsic intrusions in the Gejiu mineral district of Yunnan, China. *Computers and Geosciences*, 2010, 37(5): 662-669. <http://doi.org/10.1016/j.cageo.2010.11.001>
- [23] YALCIN MG, SETTI M, KARAKAYA F, SACCHIE E, and ILBEYLI N. Geochemical and mineralogical characteristics of beach sediments along the coast between alanya and silifke (southern Turkey). *Clay Miner*, 2015, 50(2): 233-248. <https://doi.org/10.1180/claymin.2015.050.2.07>
- [24] MCFALL B. The relationship between beach grain size and intertidal beach face slope. *Journal of Coastal Research*, 2019, 35(5): 1080-1086. <https://doi.org/10.2112/JCOASTRES-D-19-00004.1>
- [25] JOEVIVEK V. and CHANDRASEKAR N. Temporal trends of breaker waves and beach morphodynamics along the Central Tamil Nadu Coast, India. In RAMKUMAR M, JAMES RA, MENIER D, & KUMARASWAMY K. (Eds.) *Coastal Zone Management: Global Perspectives, Regional Processes, Local Issues*, 2019: 207-229. <https://doi.org/10.1016/B978-0-12-814350-6.00009-4>
- [26] UMAR H, RAHMAN S, BAEDA A.Y, and KLARA S. Identification of coastal problem and prediction of coastal erosion sedimentation in Suoth Sulawesi. *Procedia Engineering*, 2015, 116: 125-133. <https://doi.org/10.1016/j.proeng.2015.08.273>
- [27] IRFAN, U. R, KAHARUDDIN, M. S, BUDIMAN, and UMAR, H. Lithofacies analysis of Pare-Pare volcanic rocks in the Lumpue area of South Sulawesi. *Proceedings of the 43rd IAGI Annual Convention and Exhibition*, Jakarta, Indonesia, 2014.
- [28] IRZON R. Chemical composition of beach sand in southern Kulon Progo and implications for provenance. *Journal Geologi dan Sumberdaya Mineral*, 2018, 19(1): 31-45. <https://doi.org/10.33332/jgsm.geologi.v19i1.267>
- [29] BERNABEI R, MARTONE AM, ORTOLANI, E, LANDI, F, and MARZETTI, E. Screening, diagnosis and treatment of osteoporosis: a brief review. *Clinical Cases in Mineral and Bone Metabolism*, 2014. 11(3): 201-207. <https://www.ncbi.nlm.nih.gov/pmc/articles/PMC4269144/>
- [30] ABD EL-GHAFFAR M A, ABDELWAHAB NA, FEKRY AM, SANAD MA, et al. A Polyester-epoxy resin/conducting polymer/barium sulfate hybrid composite as a smart eco-friendly anti-corrosive powder coating. *Progress in Organic Coatings*, 2020, 144: 105664. <https://doi.org/10.1016/j.porgcoat.2020.105664>
- [31] MA SG, and ZHANG Y. Effect of Nb addition on the microstructure and properties of AlCoCrFeNi high-entropy alloy. *Materials Science and Engineering: A*, 2012, 532: 480-486. <https://doi.org/10.1016/j.msea.2011.10.110>
- [32] XIE W, XIONG W, MARIANETTI CA, and MORGAN D. Correlation and relativistic effects in U metal and U-Zr alloy: Validation of ab initio approaches. *Physical Review B*, 2013, 88(23): 235128. <https://doi.org/10.1103/PhysRevB.88.235128>
- [33] MAULANA A, CHRISTY AG, ELLIS DJ, and BROCKE, M. The distinctive tectonic and metamorphic history of the Barru Block, South Sulawesi, Indonesia: petrological, geochemical and geochronological evidence. *Journal of Asian Earth Science*, 2019, 172: 170-189. <https://doi.org/10.1016/j.jseaeas.2018.09.006>
- [34] ELBURG M, KAMENETSKY VS, NIKOGOSIAN I, FODEN J, and SOBOLEV AV. Coexisting High- and Low-Calcium Melts Identified by Mineral and Melt Inclusion Studies of a Subduction-Influenced Syn-collisional Magma from South Sulawesi, Indonesia. *Journal of Petrology*, 2006, 47(12): 2433-2462. <https://doi.org/10.1093/petrology/egl050>
- [35] ARMSTRONG-ALTRIN JS, NAGARAJAN R, MADHAVARAJU J, ROSALEZ-HOZ L, et al. Geochemistry of the jurassic and upperCretaceous shales from the olango Region, Hidalgo, Eastern Mexico: implications of source-area weathering, provenance, and tectonic setting. *Comptus Rendus Geoscience*, 2013, 345(4): 185-202. <http://dx.doi.org/10.1016/j.crte.2013.03.004>
- [36] HOOD SB, CRACKNELL MJ, GAZLEY MF, and READING AM. Element mobility and spatial zonation associated with the archean hamlet orogenic Au deposit, Western Australia: Implications for fluid pathways in shear zones. *Chemical Geology*, 2019, 514: 10-26. <https://doi.org/10.1016/j.chemgeo.2019.03.022>
- [37] TONGGIROH A, KAHARUDDIN, and MAULANA, B. R. Geochemical analysis of dacite rocks in Barru area, South Sulawesi. *Proceedings of the 43rd IAGI Annual Convention and Exhibition*, South Sulawesi, 2014. <http://repository.unhas.ac.id/handle/123456789/17699>

- [38] MELFOS V, and VOUDOURIS P. Cenozoic metallogeny of Greece and potential for precious, critical and rare metals exploration. *Ore Geology Reviews*, 2017, 89: 1030-1057. <https://doi.org/10.1016/j.oregeorev.2017.05.029>
- [39] RANASINGHE R, CALLAGHAN D, and STIVE MJF. A process based approach to derive probabilistic estimates of coastal recession due to sea level rise. In MIZUGUCHI M, and SATO S. (Eds.) *Proceedings of the 6th International Conference on Coastal Dynamics*, Japan, 2009: 1-9. http://dx.doi.org/10.1142/9789814282475_0133
- [40] IRFAN UR, and AKBAR A. Determination of Geochemical Correlation of Cu, Pb, Zn in Stream Sediment Samples in Barru Area, South Sulawesi. *Proceedings of the 3rd EPI International Conference on Science and Engineering*, South Sulawesi, Indonesia, 2019: 875. <https://doi.org/10.1088/1757-899X/875/1/012049>
- [41] HOSSAIN HMZ, KAWAHATA H, ROSER BP, SAMPEI Y, et al. Geochemical characteristics of modern river sediments in Myanmar and Thailand: Implications for provenance and weathering. *Geochemistry*, 2017, 77(3): 443-458. <https://doi.org/10.1016/j.chemer.2017.07.005>
- [42] TONGGIROH A, FARIDA M, SIRAJUDDIN H, and BATTU DP. Characteristic sulfat geochemistry of barite (BaSO₄) Marine type on marl tonasa formation Barru, South Sulawesi. *Materials Science Engineering*, Gowa, Indonesia, 2019: 676. <https://doi.org/10.1088/1757899X/676/1/012034>
- [43] TAYLOR SR, MCLENNAN SM, & MCCULLOCH MT. Geochemistry of loess, continental crustal composition and crustal model ages, *Geochimica et Cosmochimica Acta*, 1983, 47(11): 1897-1905. [https://doi.org/10.1016/0016-7037\(83\)90206-5](https://doi.org/10.1016/0016-7037(83)90206-5).
- [44] SENGUPTA D and GOSEN BS. Placer-Type rare earth element deposits. In VERPLANCK PL, & HITZMAN MW. *Rare Earth and Critical Elements in Ore Deposits*. Society of Economic Geologists, 2016, 18: 81-100. <https://doi.org/10.5382/Rev.18.04>
- 参考文献:**
- [1] MALICK B M L、YOUNG L M 和 ISHIGA H。日本九州北部海滩沙的主量和微量元素地球化学。岛根大学地球科学报告, 2012, 31 : 1-8。
- [2] MALICK B M L, 和 ISHIGA H。日本西南部山阴地区袖珍海滩沙的地球化学成熟度。地球科学研究, 2015, 4 : 74-84。 <http://dx.doi.org/10.5539/esr.v4n2p74>
- [3] ALYAZICHI Y M、JONES BG、MCLEAN E、PEASE J 和 BROWN H。澳大利亚悉尼南部乔治河表层沉积物中微量元素污染的地球化学评估。环境污染与毒理学档案, 2017, 72 : 247-259。 <https://doi.org/10.1007/s00244-016-0343-z>
- [4] LONG K R, VAN GOSEN BS, FOLEY NK, 和 CORDIER D。美国主要稀土元素矿床: 国内矿床总结和全球视角”。在: SINDING-LARSEN R, WELLMER FW。(编辑) 不可再生资源问题。国际地球年。施普林格, 多德雷赫特, 2012。 https://doi.org/10.1007/978-90-481-8679-2_7。
- [5] WITASARI, Y.印度尼西亚望加锡海峡近期沉积物中粘土矿物和微量元素的组成和来源。第十三届国际科学技术研究会议论文集。印度尼西亚巴厘岛, 2454-5880, 2018。
- [6] MAULANA A, CHRISTY A G, 和 ELLIS D J。印度尼西亚苏拉威西岛南臂蛇纹石化超镁铁岩的岩石学、地球化学和构造意义。地球化学-地球化学。2014, 75(1): 73-87。 <https://doi.org/10.1016/j.chemer.2014.09.003>
- [7] GODANG S、IDRUS A、FADLIN BP 和 BASUKI NI。印度尼西亚西苏拉威西岛 65 号钻芯火山风化层中稀土元素的腐泥化特征。亚洲应用科学杂志, 2019, 7(4): 435-450. <http://dx.doi.org/10.24203/ajas.v7i4.5873>
- [8] WAKITA K, MUNASRI SOPAHEL UWAKA NJ, ZULKARNAEN I, 和 MIYAZAKI K. 印度尼西亚南苏拉威西班蒂马拉地区放射虫燧石年龄与其变质基底之间的时间滞后所暗示的早白垩世构造事件。岛弧, 1994, 3 : 90-102。 <https://doi.org/10.1111/j.1440-1738.1994.tb00097.x>
- [9] YOUNG S M、PITAWALA A 和 ISHIGA H。斯里兰卡马哈威利河及其流域的河流沉积物、沉积物组分、土壤和基岩的地球化学特征。地球化学, 2013, 73 : 357-371。 <https://doi.org/10.1016/j.chemer.2012.09.003>
- [10] O'SULLIVAN G、CHEW D、KENNY G、HENRICH I 和 MULLIGAN D。磷灰石的微量元素组成及其在碎屑来源研究中的应用。地球科学评论, 2020, 201 : 103044。 <https://doi.org/10.1016/j.earscirev.2019.103044>
- [11] JORDENS A、CHENG YP、WATERS KE。含稀土矿物选矿综述。矿物工程, 2013, 41 : 97-114。 <https://doi.org/10.1016/j.mineng.2012.10.017>
- [12] ACHARYA BC、NAYAK B K 和 DAS S K。印度奥里萨邦甘贾姆区孔蒂亚加尔地区重矿物砂矿床。资源地质, 2008, 59(4): 388-399. <https://doi.org/10.1111/j.1751-3928.2009.00105.x>
- [13] HOU B, KEELING J.和 GOSEN B S. 海滩砂矿沉积物的地质和勘探模型, 综合澳大利亚南部的案例研究。矿物地质评论, 2017, 80 : 437-459。 <https://doi.org/10.1016/j.oregeorev.2016.07.016>
- [14] PAPAPOPOULOS A、TZIFAS IT 和 TSIKOS H。希腊沿海砂矿床中稀土元素和相关关键金属的潜力。矿物, 2019, 9(8) : 469。 <https://doi.org/10.3390/min9080469>
- [15] CHARLESWORTH S、DE MIGUEL E 和 ORDONES A。城市陆地环境中颗粒微量元素分布及其在风险考虑中的应用的综述。环境地球化学与健康, 2011, 33(2): 103-123. <https://doi.org/10.1007/s10653-010-9325-7>。
- [16] NAMAYANDEH A、MODABBERI S 和 LOPEZ-GALINDO A。伊朗东部膨润土矿床中火山灰成膨润土成岩蚀变过程中的痕量和稀土元素分布和迁移率。粘土和粘土矿物, 2020, 68(1) : 50-66。 <https://doi.org/10.1007/s42860-019-00054-9>
- [17] SITDIKOVA LM、IBRAGIMOV EA、BADRUTDINOV OR、KHASANOVA NM 和 MUKHAMATDINOV, I. I. 阿拉伯海岸(印度喀拉拉邦奎隆)沿海海洋砂矿沉积物的物质成分。国际多学科科学地理会议: SGEM, 2016, 1 : 361-367。
- [18] PRAKASH T、BLACK K、MATHEW J、KURIAN NP 等人。印度西南部以砂矿为主的海岸的近岸和海滩沉积动力学。海岸研究杂志, 2007, 23(6) : 1391-1398。 <http://www.jstor.org/stable/30138538>。
- [19] PISIAS NG、MURRAY RW 和 SCUDDER RP。沉积地球化学数据集的多元统计分析和划分: 一般原则和特定 MATLAB 脚本: 技术简介。地球化学、地球物理学

- 、地球系统, 2013, 14(10): 4015-402. <https://doi.org/10.1002/ggge.20247>
- [20] ALBANESE, S、CICCHELLA, D 和 DE VIVO, B. 城市地区地球化学测绘, 第 8 章, 环境地球化学场地特征、数据分析和案例历史, 2017。 <http://dx.doi.org/10.1016/B978-0-444-63763-5.00009-4>
- [21] IWAMORI H, YOSHIDA K, NAKAMURA H, KUWATANI T, 等。基于多元统计分析的地球化学数据分类: 聚类分析、主成分分析和独立成分分析的互补作用。地球化学、地球物理学、地球系统, 2017, 18: 994-1012。 <https://doi.org/10.1002/2016GC006663>
- [22] CHENG Q, CARTER G. B, WANG, W, ZHANG, S, LIE, W, 和 QINGLIN, X. 个旧矿区长英质侵入体多元素地球化学数据的空间加权主成分分析 中国云南。计算机与地球科学, 2010, 37(5): 662-669. <http://doi.org/10.1016/j.cageo.2010.11.001>
- [23] YALCIN MG、SETTI M、KARAKAYA F、SACCHIE E 和 ILBEYLI N. 阿拉尼亚和锡利夫克(土耳其南部)之间海岸海滩沉积物的地球化学和矿物学特征。粘土矿工, 2015, 50(2): 233-248。 <https://doi.org/10.1180/claymin.2015.050.2.07>
- [24] MCFALL B. 海滩粒度与潮间带海滩坡度的关系。海岸研究杂志, 2019, 35(5): 1080-1086。 <https://doi.org/10.2112/JCOASTRES-D-19-00004.1>
- [25] JOEVIVEK V. 和 CHANDRASEKAR N. 印度泰米尔纳德邦中部海岸碎波和海滩形态动力学的时间趋势。载于 RAMKUMAR M、JAMES RA、MENIER D 和 KUMARASWAMY K. (编辑) 沿海地区管理: 全球视角、区域进程、地方问题, 2019: 207-229。 <https://doi.org/10.1016/B978-0-12-814350-6.00009-4>
- [26] UMAR H, RAHMAN S, BAEDA A.Y, 和 KLARA S. 苏拉威西海岸问题识别及海岸侵蚀沉积预测。普罗塞迪工程, 2015, 116: 125-133。 <https://doi.org/10.1016/j.proeng.2015.08.273>
- [27] IRFAN, U. R, KAHARUDDIN, M. S, BUDIMAN, 和 UMAR, H. 南苏拉威西伦普埃地区帕雷帕雷火山岩岩相分析. 2014 年印度尼西亚雅加达第 43 届国际航空工业协会年度大会暨展览会论文集。
- [28] IRZON R. 库隆普罗戈南部海滩沙的化学成分及其对来源的影响。矿物地质学报, 2018, 19(1): 31-45. <https://doi.org/10.33332/jgsm.geologi.v19i1.267>
- [29] BERNABEI R、MARTONE AM、ORTOLANI, E、LANDI, F 和 MARZETTI, E. 骨质疏松症的筛查、诊断和治疗: 简要回顾。矿物质和骨代谢临床病例, 2014。11(3): 201-207。 <https://www.ncbi.nlm.nih.gov/pmc/articles/PMC4269144/>
- [30] ABD EL-GHAFFAR M A、ABDELWAHAB NA、FEKRY AM、SANAD MA 等。A. 聚酯环氧树脂/导电聚合物/硫酸钡杂化复合材料作为智能环保防腐粉末涂料。有机涂料进展, 2020, 144: 105664。 <https://doi.org/10.1016/j.porgcoat.2020.105664>
- [31] MA SG, ZHANG Y. 铈添加对铝钴铬铁镍高熵合金组织与性能的影响。材料科学与工程: A, 2012, 532: 480-486。 <https://doi.org/10.1016/j.msea.2011.10.110>
- [32] XIE W, XIONG W, MARIANETTI CA, 和 MORGAN D. U 金属和铀合金中的相关性和相对论效应: 从头计算方法的验证。物理评论乙, 2013, 88(23): 235128. <https://doi.org/10.1103/PhysRevB.88.235128>
- [33] MAULANA A, CHRISTY AG, ELLIS DJ, 和 BROCKE, M. 印度尼西亚南苏拉威西岛巴鲁地块独特的构造和变质历史: 岩石学、地球化学和地质年代学证据。亚洲地球科学学报, 2019, 172: 170-189. <https://doi.org/10.1016/j.jseaeas.2018.09.006>
- [34] ELBURG M、KAMENETSKY VS、NIKOGOSIAN I、FODEN J 和 SOBOLEV AV. 通过对印度尼西亚南苏拉威西岛受俯冲影响的同步碰撞岩浆的矿物和熔体包裹体研究鉴定出共存的高钙和低钙熔体。岩石学报, 2006, 47(12): 2433-2462. <https://doi.org/10.1093/petrology/egl050>
- [35] ARMSTRONG-ALTRIN JS、NAGARAJAN R、MADHAVARAJU J、ROSALEZ-HOZ L 等。墨西哥东部伊达尔戈州奥兰戈地区侏罗系和上白垩统页岩的地球化学: 源区风化、物源和构造环境的影响。康图斯地球科学, 2013, 345(4): 185-202. <http://dx.doi.org/10.1016/j.crte.2013.03.004>
- [36] HOOD SB、CRACKNELL MJ、GAZLEY MF 和 READING AM. 与西澳大利亚太古代小村庄造山金矿床相关的元素流动性和空间分带: 对剪切带流体路径的影响。化学地质, 2019, 514: 10-26. <https://doi.org/10.1016/j.chemgeo.2019.03.022>
- [37] TONGGIROH A, KAHARUDDIN, 和 MAULANA, B. R. 南苏拉威西省巴鲁地区英安岩的地球化学分析. 第 43 届国际航空工业协会年度大会暨展览会论文集, 南苏拉威西, 2014。 <http://repository.unhas.ac.id/handle/123456789/17699>
- [38] MELFOS V 和 VOUDOURIS P. 希腊新生代成矿学以及贵重、关键和稀有金属勘探的潜力。矿石地质评论, 2017, 89: 1030-1057。 <https://doi.org/10.1016/j.oregeorev.2017.05.029>
- [39] RANASINGHE R, CALLAGHAN D, 和 STIVE MJF. 一种基于过程的方法, 用于对海平面上升导致的沿海衰退进行概率估计。载于 MIZUGUCHI M 和 SATO S. (编) 第六届国际海岸动力学会议记录, 日本, 2009: 1-9。 http://dx.doi.org/10.1142/9789814282475_0133
- [40] IRFAN UR, 和 AKBAR A. 南苏拉威西岛巴鲁地区河流沉积物样品中铜、铅、锌地球化学相关性的测定。第三届 EPI 国际科学与工程会议论文集, 印度尼西亚南苏拉威西, 2019: 875。 <https://doi.org/10.1088/1757-899X/875/1/012049>
- [41] HOSSAIN HMZ、KAWAHATA H、ROSER BP、SAMPEI Y 等。缅甸和泰国现代河流沉积物的地球化学特征: 对来源和风化的影响。地球化学, 2017, 77(3): 443-458. <https://doi.org/10.1016/j.chemer.2017.07.005>
- [42] TONGGIROH A、FARIDA M、SIRAJUDDIN H 和 BATTU DP. 南苏拉威西岛泥灰岩托纳萨地层巴鲁重晶石(硫酸钡)海相类型的硫酸盐地球化学特征。材料科学与工程, 戈瓦, 印度尼西亚。2019: 676。 <https://doi.org/10.1088/1757899X/676/1/012034>
- [43] TAYLOR SR, MCLENNAN SM, 和 MCCULLOCH MT. 黄土地球化学、大陆地壳成分和地壳模型年龄, 地球化学与宇宙化学学报, 1983, 47(11): 1897-1905. [https://doi.org/10.1016/0016-7037\(83\)90206-5](https://doi.org/10.1016/0016-7037(83)90206-5)
- [44] SENGUPTA D 和 GOSEN BS. 砂矿型稀土元素矿床。在 VERPLANCK PL 和 HITZMAN MW. 矿床中的稀土和关键元素。经济地质学会, 2016, 18: 81-100。 <https://doi.org/10.5382/Rev.18.04>